10.26411/83-1734-2015-2-56-17-24

Experimental Studies of a Soil Wedge of the Physical Model of a Retaining Wall Made with Reinforced Soil

Zenon Zamiar
The International University of Logistics and Transport in Wroclaw

Andrzej Surowiecki
The International University of Logistics and Transport in Wroclaw

Abstract
The subject of this article concerns the problem of estimating the area of a breakaway wedge in a massif with a vertical retaining wall of reinforced soil, in which a boundary active thrust condition has been induced. The auxiliary parameter sought is the slip line, which cuts off from the plane of the retaining wall the sought soil wedge. The presented research method makes it possible to estimate the reduction of the area of the wedge of detachment in a reinforced massif, in comparison to an identical structure without reinforcement. The task is solved using physical high-dimensional models loaded vertically in a static manner. The object of the study is to measure the horizontal displacements of the massif models and the relative deformations of the reinforcement inserts. The following have been presented: the research site, the measurement technique and the method of estimating the location of the slip surface.

Key words: reinforced soil, retaining structure, soil wedge, physical models

1. PURPOSE AND SUBJECT MATTER OF RESEARCH

The classic reinforced soil, which is a French invention (Laboratoire Central des Ponts et Chaussées – LCPC) [1, 3, 10-12, 16] has found its widest application in the field of retaining structures, among others, as the structures for harbour quays, retaining walls at unstable slopes (embankments or communication cuts), and bridge abutments [2, 4-9, 13-15].

When designing reinforced soil retaining structures, the necessary length of each reinforcement insert is calculated as the sum of the lengths in the push zone and in the anchorage zone. The line of maximum tensile forces (the so-called slip line) divides the soil mass into the these two zones. As a result, the slip line cuts off the so-called soil wedge from the plane of the retaining wall. In engineering practice, the length of the push zone L_{pz} is determined approximately as follows [6, 18]:

- for z depth = 0,0÷0,50 H measured from the top surface of the soil massif L_{pz} = 0,3 H (H is the height of the massif above the surface),
- for z > 0,5 H, the L_{pz} length is to be calculated with the use of the Coulomb's soil wedge [21].

Therefore, the way in which the shape of the line dividing the massif into two zones (i.e., the slip line) is adopted has an impact on the economics of reinforcement.

The present article addresses the topic of estimating the area of the soil wedge in a reinforced and unreinforced (reference) massif, given a high-dimensional physical model.

The overall objective of the study is to estimate the size of the breakaway wedge in a physically modelled retaining structure. A supporting task was the search for a slip line, cutting off the sought soil wedge from the plane of the retaining wall. The final effect was the estimation of the degree of reduction of the soil wedge in the reinforced mass (depending on the type of reinforcement inserts) in relation to an identical structure without reinforcement.

It should be emphasised that, in terms of theoretical analyses and experimental studies, the subject in question is recognised in quite some detail [2, 4, 5, 7-9, 14, 15]. However, the bases developed (as a result of advanced research and analysis) for the functioning of reinforced soil as a material forming engineering structures are in many cases rooted in simplifying assumptions. It is therefore justified to continue the experimental research in which the relationships between the parameters characterising the interaction process between the soil medium (constituting the matrix) and the reinforcing inserts are determined by direct measurement. Thus, the present article presents an approach to analyse the performance of the reinforced soil on the basis of research tests performed on physical models on a laboratory scale. The adopted test method allows the relative determinateness of the experimental conditions to be maintained and one of the parameters sought to be changed in a programmed manner, while keeping the others unchanged [17-20].

The subject of the study is the measurement of:
- horizontal displacements y_{ik} of the loaded soil massif, performed in the plane of the retaining wall of the model,
- relative deformations ε in the reinforcement inserts, using the electrical resistivity strain gauge method.

On the basis of the values of displacements y_{ik}, the horizontal soil pressure on the retaining wall $p_{y,ik}$ was calculated using the transformation formula $p_{y,ik} = C_s \cdot y_{ik}$, where C_s [kN/m^3] is the elasticity constant of the elementary pressure sensor of the retaining wall [17, 18].

2. OBJECT OF STUDY, METHOD AND TEST SITE

The study object is a physical model of a massif with a vertical wall of reinforced soil contained within a rectangular steel container (Fig. 1 and 2) [17, 18]. The necessary length of the container L in relation to the height H was designed according to K. Terzaghi's method ($L = H \cdot \text{ctg}\, \varphi$, where φ is the angle of internal soil friction) assuming that the active pressure of the soil in the range covering all phases, up to the boundary condition, is studied. The construction of one of the front walls (the so-called retaining measurement wall) allows for the movement of the ground medium and the measurement of the horizontal component of the linear displacement of the ground massif, which is the measure of the active pressure. Permanent contact between the retaining wall and the pushing soil material is ensured during the individual phases of the test. In the limit state of active soil pressure, a slip line is formed, which separates the fragment block (the so-called wedge) from the remaining (stationary) part of the soil massif. The wedge is the factor that generates the ground pressure on the plane of the retaining wall.

The soil material filling the test container is dry, coarse sand, characterised by the physical parameters of [18]: volumetric weight when loosely poured γ_0 = 19,0 kN/m^3, natural humidity w_n = 0,3%, degree of compaction when loosely poured I_D = 0,38, and the angle of internal friction $\varphi = 30{,}2^0$ (indicated for a sand sample in a laboratory-based, direct shear apparatus).

Reinforcement inserts in the form of "flaccid" tapes with a length l_a = 1,80 m and a cross-section b_a x g_a = 0,024 m x 0,001 m (b_a – width, g_a – thickness) were used [18, 20]. The inserts, made of hardened spring steel with the symbol 50HSA (characterised by a longitudinal modulus of elasticity of E = 210437,7 MPa) were arranged in

horizontal layers with a vertical spacing of e_z = 0,195 m. The following reinforcement systems are considered (differing in terms of the configuration of inserts):
A → 5 layers of reinforcement, 9 inserts with a length of 1.80 m in the layer;
B → 5 layers of reinforcement, 6 inserts with a length of 1.80 m in the layer;
C → 5 layers of reinforcement, 4 inserts with a length of 1.80 m in the layer;
D → 2 layers of reinforcement, 9 inserts with a length of 1.80 m in the layer;
E → 2 layers of reinforcement, 9 inserts with a length of 1.30 m in the layer;
F → 2 layers of reinforcement, 9 inserts with a length of 1.00 m in the layer;
G → 2 grids with a length of 1.80 m made with the use of perpendicularly crossed tapes, arranged in levels z_1 and z_2.

Horizontal spacing of straps: e_x = 0,11 m, mesh size of grating: $e_x = e_y$ = 0,11 m.

The models were reinforced with two types of tapes: with a smooth surface and with a "rough" surface. The "roughness" of the surface of the tapes was obtained by attaching special "notches" in the form of steel angle irons on both sides (by means of electric welding) (Fig. 3). These angle irons, by spatially shaping the surface of the tapes, ensure that the resistance of the inserts to displacement in the soil medium is increased.

One of the intermediate stages of the study was the determination of the normal tensions in the reinforcement inserts, via strain gauge unit strain measurements. Therefore, the use of "flaccid" inserts guaranteed the initiation of measurable strain ε. The location of the strain gauges along the length of the tapes was designed to cover mainly the active zone (i.e., the extent of the fracture wedge) and partly the anchorage zone. The strain gauges were coated with resin to protect them from mechanical damage and moisture. Strain gauge readings were measured and recorded using a multi-point, automatic strain test set-up, consisting of a set of equipment: an automatic strain gauge bridge, a control module for measuring and connecting strain gauges, strain gauge boxes and a microcomputer with a printer.

The primary objective of the study was to estimate the position of the slip line (assuming a two-dimensional system of the model) at the limit state of active thrust in the ground mass. The slip line was obtained as the geometric location of the maximum normal tensions along the inserts, located at each of the five measurement levels of the model. The tension values were expressed by the classic Hooke's law $\sigma = E \cdot \varepsilon$.

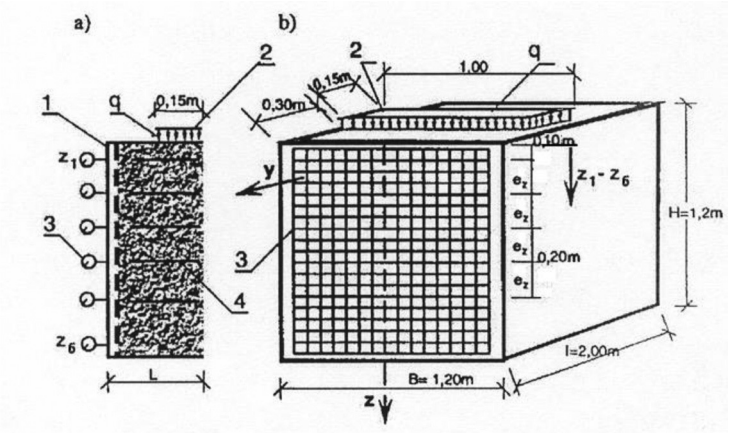

Fig. 1. Model of the reinforced soil massif [17, 18]: *a* – a piece of vertical longitudinal section, *b* – general view, *1* – retaining (measuring) wall of the model, *2* – weight plate measuring 0,15 x 1,0 m; *3* – horizontal displacement sensors, *4* – reinforcement inserts; z_1, z_2, z_3, z_4, z_5, z_6 – levels of measurement

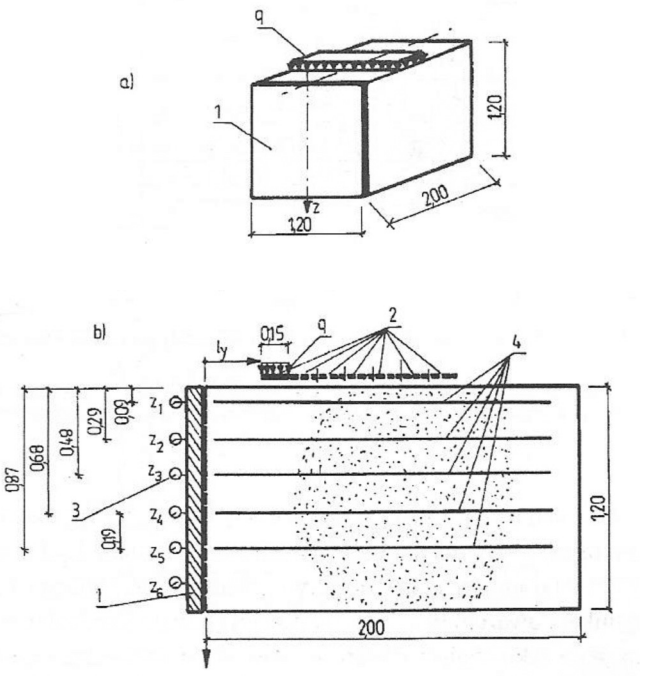

Fig. 2. Research site [17, 18]: *a* – general view (scheme), *b* – vertical longitudinal section, *1, 2, 3, 4* – symbols as on the Fig.1.; l_y – the distance of the plate from the reinforcement wall

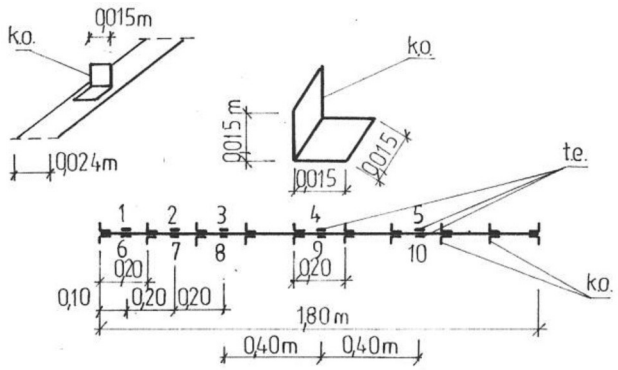

Fig. 3. Reinforcement insert with retainment elements in the form of angle irons [17, 18]: *t.e.* – electrofusion strain gauges installed on the plate's surface (no. 1-5) and on the lower one (no. 6 -10), *k.o.* – reinforcement angle irons

The horizontal pressure of the soil massif (in the range from the value referred to as resting pressure in the loosely packed soil state to the value of limiting active pressure), causing displacements of the retaining wall surveying elements, is induced by a special vertical band load. The designed load on the soil massif model results from the test method and is mainly the initiating factor for the generation of the breakout block. It should be regarded as approximate, but within acceptable limits. The loading was implemented statically, via a 0.15 x 1.0 m steel plate located horizontally on the model floor, transverse to the longitudinal axis of the model (Fig. 1, 2). The minimum distance of the edge of the plate from the inner surface of the measuring wall is taken as l_y = 0,30 m. The load value (in the range of 0-61,69 kPa) was applied uniformly for all tests and was minimum but necessary to produce a lump of debris in the soil mass model.

Two states of compaction of the soil massif were analysed: loosely poured (*l.s.*) and pre-densified on the surface (*w.z.p.*). The method of testing consisted in analysing the process of changes in the value of the horizontal soil pressure on the retaining wall, as the loading plate was moved in the direction opposite to the wall.

3. SYNTHESIS OF RESEARCH RESULTS

The elaboration of research results addressed the following problems:

- distribution of horizontal pressure of the soil mass on the $p_{y,ik}$ retaining wall as a function of variable parameters of the reinforcement inserts and the soil medium,

- the process of disappearance of the influence of the model floor load q on the value of the horizontal massive pressure in the plane of the retaining wall $p_{y,ik}$ in view of the progressive increase in the distance of the loading plate from this wall l_y (Fig. 2*b*).
- the value and distribution of normal tensions in the reinforcement inserts, depending on the location of the loading plate, characterized by the parameter l_y.

Based on the analysis of the course of the phenomenon of the disappearing horizontal push of the massif in the plane of the retaining wall, as the distance of the loading plate from this wall increases l_y (Fig. 2*b*), the horizontal length of the zone of influence of the actions of the loaded massif on the state of horizontal thrust in the plane of the wall was estimated. This length was treated as the extent of the wedge of detachment. The slip line from the analysis of this phenomenon at the different measurement levels of the modelled massif was also determined (z_1, …, z_6). The totality of the issues presented can be described as a search for the maximum volume and shape of the soil massif pushing against the retaining wall due to the applied "research" loading of the massif floor. The course of the slip line was verified by determining the geometric place of the maximum tensile forces in the individual layers of reinforcement using the method of electrical resistivity strain gauging.

Figure 4 presents the process of the soil pressure p_y^q on the retaining wall of the model, induced by the test load q = 61,69 kPa as a function of the change in the position of the loading plate l_y in relation to the retaining wall. The length of the zone of influence of load q on the value of ground pressure in the plane of the retaining wall is not the same at the different measurement levels of the model z_1, …, z_6. As the parameter l_y increases, the influence of the load q is reduced until it disappears completely. The location of the loading plate in this characteristic case is denoted as $l_y = l_{y,liminal}$. The segment $l_{y,liminal}$ is shorter in a precompacted massif (whose angle of internal friction φ is greater). The position of the load plate $l_y > l_{y,liminal}$ is not accompanied by any increments in the soil pressure on the wall if a test load of any value is to be introduced. Figures 5 and 6 show the course of the phenomenon in question (the disappearance of the effect of the load q on the value of the soil pushover in the example measurement level of the retaining wall z_1 = 0,095 m), taking into account different reinforcement systems.

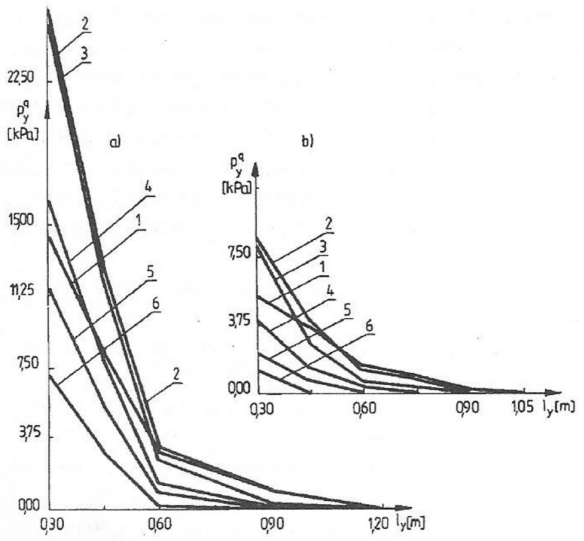

Fig. 4. The course of the unit soil pressure p_y^q [kPa] generated by the research loading q = 61,69 kPa within the load plate displacements function l_y [18]:
a – loosely poured, non-reinforced massif,
b – pre-densified, non-reinforced massif ; *1,…6* – soil pressure levels p_y^q for individual measuring levels of the retaining wall of the model

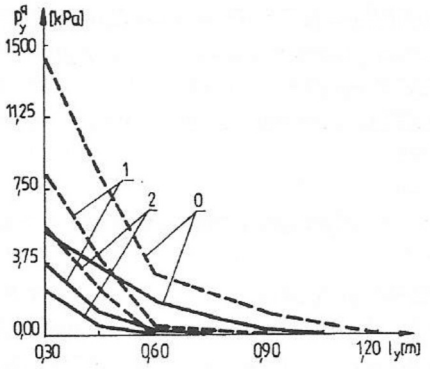

Fig. 5. Unit soil pressure p_y^q [kPa], measured at the level of measurement z_1 = 0,095 m with research loading q = 61,69 kPa [18]. Markings:
- - - loosely poured massif,
- pre-densified, *0* – non-reinforced (template), *1* – notch-less tape reinforcement (the A system),*2* – notched-tape reinforcement (the A system)

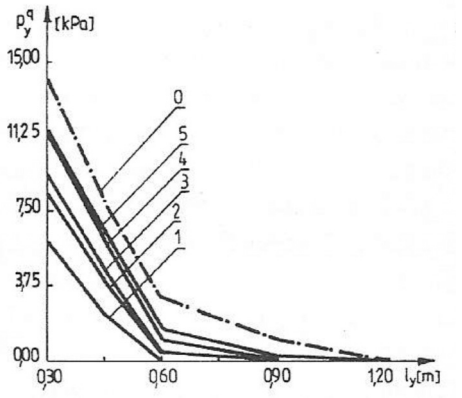

Fig. 6. Unit soil pressure p_y^q [kPa], measured at the level of measurement z_1 = 0,095 m With research loading q = 61,69 kPa [18]. Loosely poured massif. Markings: *0* – non-reinforced, *1* – system G, *2* – notch-less tapes in the A system, *3* – notch-less tapes in the D system, *4* – notch-less tapes in the E system, *5* – notch-less tapes in the F system

The length of the zone of influence $l_{y,liminal}$ (and the size of the wedge of detachment associated with this parameter) in reinforced soil is smaller than in unreinforced soil and depends on the number of inserts and the quality of the reinforcement's interaction with the soil.

Figure 7 illustrates the change in the experimentally determined approximate size of the soil wedge (characterised by the parameter $l_{y,liminal}$) in a reinforced and unreinforced (reference) mass. The approximate value of $l_{y,liminal}$ results from the conditions accompanying the test method: e.g., constant measurement interferences, the applied transfer interval Δl_y of the loading band. The individual curves no. 1÷6 (Fig. 7) has been approximated with the use of the functions:

- curve 1: $v = ae^{bu}$, coefficient a = 3,788·10^{-2}, coefficient b = 3,587; correlation coefficient C_c = 0,988;
- curve 2: $v = ae^{bu}$, a = 6,159·10^{-3}, b = 4,464; C_c = 0,997;
- curve 3: $v = ae^{bu}$, a = 1,053·10^{-2}, b = 6,119; C_c = 0,988;
- curve 4: $v = ae^{bu}$, a = 1,085·10^{-3}, b = 11,221; C_c = 0,974;
- curve 5: $v = ae^{bu}$, a = 2,063·10^{-4}, b = 15,431; C_c = 0,963;
- curve 6: $v = ae^{bu}$, a = 4,573·10^{-5}, b = 21,806; C_c = 0,972.

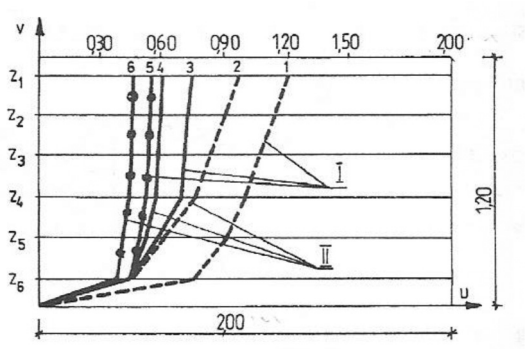

Fig. 7. Experimentally estimated zone of the soil wedge $l_{y,liminal}$ and the course of the slip line [18].Markings: - - - non-reinforced massif, --- massif reinforced with notch-less tapes in the A system,-·-·- reinforced with notched tapes in the A system A, *I* – loosely poured massif,*II* – pre-densified on the surface, *v* – vertical coordinate, *u* – horizontal coordinate

The reduction rate of the soil wedge $W_{r,ko}$ as a result of the installation of reinforcement inserts is described by the relationship:

$$W_{r,ko} = [100 - A_{ko}^{*} (A_{ko})^{-1}] \cdot 100 \ [\%] \tag{1}$$

where:

A_{ko}^{*}, A_{ko} – the surfaces of the soil wedge in the reinforced and non-reinforced massif, respectively.

The total pressure of the soil mass contained in the detachment wedge $P_{y,ko}$ equal to the mass of the detachment wedge M_{ko} is the function of at least several variables (assuming the reinforcement of the mass with inserts located in the horizontal layers):

$$P_{y,ko} = M_{ko} = f\,[(n_a^{w})^{-1}, (R_r)^{-1}, (F_{col})^{-1}, (\varphi)^{-1}] \tag{2}$$

where:

n_a^{w} – number of inserts within a layer,
R_r – tensile strength of the reinforcement,
F_{col} – reinforcement-soil cooperation index,
φ – internal friction angle of the soil.

From the literature (e.g., F. Schlosser [10, 12]) on experimental studies of horizontally reinforced soil, it is known that the potential slip curve in the state of boundary equilibrium state of strain gauging can be obtained graphically. It is the geometrical

location of the maximum tensile forces that occur in the reinforcement inserts. Proceeding analogously to the locations along the length of the inserts where the highest values of strain gauging were obtained by electrofusion strain gauging, the slip curve was determined experimentally (Fig. 8). The accuracy of the estimate is owing to, among others, the number of strain gauge locations and their distribution on the surface of the inserts.

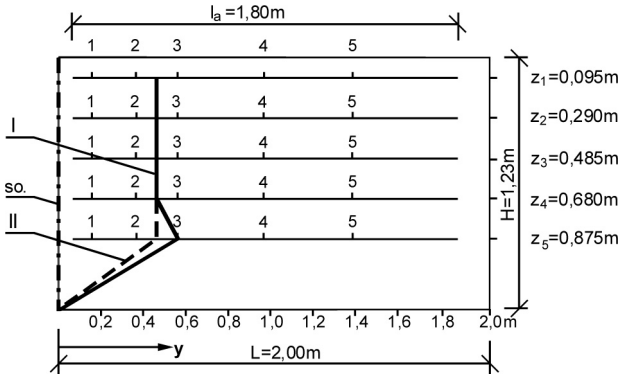

Fig. 8. Slip lines as the curves which connect the maximum strain gauging points within the reinforcement [18]. Approximately estimated on the basis of tensometric measurements. Markings: *1÷5* – numbers of strain gauges applied on the top surfaces of the inserts, $z_1 \div z_5$ – measurement levels where the reinforcement inserts are located; *I* – loosely poured massif reinforced with notched tapes (the A system of reinforcement), *II* – pre-densified massif reinforced on the surface like *I*, s.o. – retainment wall

French studies (e.g., [11]) show that in a massif with a vertical wall of reinforced soil, whose floor is loaded, the distribution of strain gauging in the reinforcement from the dead weight of the structure and from the service load has the same character as in unloaded massifs. In view of this, the research concept developed by the authors of this article – consisting in the introduction of a special test loading of the model floor (with a value of q being the minimum necessary) in order to induce such a value of soil pressure that will generate the formation of a break wedge – is oriented correctly.

Studies [11] have also proved that the position of the line of maximum strain gauging (separating the active zone from the soil resistance zone [1IMG]) in a massif with an externally loaded floor can be different from that in an unloaded one (Fig. 9). It depends on the ratio of the magnitude of the external load Q to the weight of the massif. However, N. T. Long [11] does not give an exact value for this quotient,

operating only with the expression: "high and low loading". The course of curve (*1*) in Figure 9*b* is similar to the slip line obtained by the authors in the process of strain gauge testing (Fig. 8). As previously mentioned, the special study load was selected by means of tests and has a value as low as possible, at which the objective of the task is achieved while taking into account a number of technical constraints.

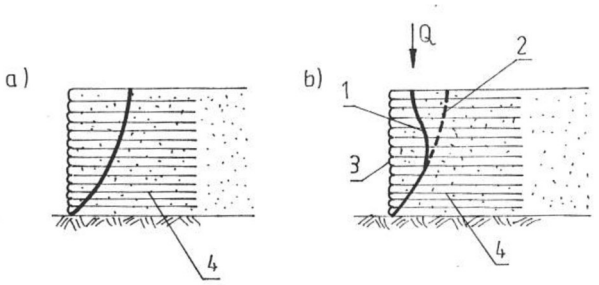

Fig. 9. Lines connecting the points of maximum strain gauging within the reinforcement. A theoretical model – the calculation results obtained with the use of finite element method [11].Markings: *a* – non-loaded soil, *b* – loaded-soil, *1* – substantial loading, *2* – insubstantial loading, *3* – vertical wall of the massif, *4* – reinforcement inserts

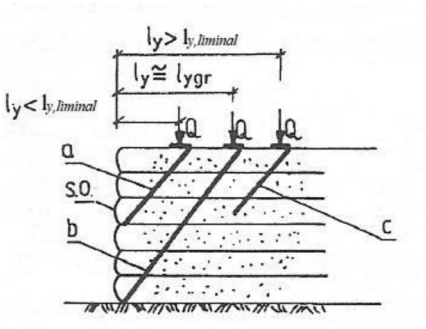

Fig. 10. Ways of destruction of reinforced soil massif depending on the location of the loading strip on the massif's surface (according to [11]): *s.o.* – outer, curtain wall, $l_{y,liminal}$ – the liminal localisation of the loading strip

N. T. Long's research [11] on two-dimensional models on a small scale showed that the way of destruction of a massif due to an increase in the value of the service load uniformly distributed on the floor along the length of the massif depends on the distance l_y of the load band from the plane of the outer-curtain wall (Fig. 10). If the distance l_y is less than the limit value $l_{y,liminal}$, then the soil wedge of detachment

appears, limited to the upper part of the massif (line *a*). The destruction is progressive: it starts near the outer wall and ends at the point of load application. In the case of a distance $l_y \approx l_{y,liminal}$, the slip surface reaches the edge of the base of the massif (line *b*). When the distance of the loading band from the wall plane is increased beyond $l_{y,liminal}$, the influence of the outer wall becomes negligible and the failure caused by the service load takes the form of the so-called punctures of the reinforced massif (line *c*). Then the failure starts at the upper surface of the massif and deepens with increasing load values *Q*.

4. CALCULATION SCHEMES FOR REINFORCED SOIL STRUCTURES

Modern reinforced soil structures are designed using the limit state method. A calculation scheme for these structures is shown in Figure 11 [6, 13]. Four types of stability of the reinforced soil mass are required to be checked [6, 13]: external, internal, general and stability due to the bearing capacity of the ground.

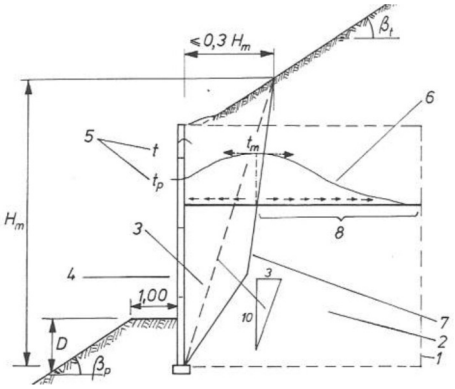

Fig. 11. Calculation scheme of the reinforced soil construction [6, 13]: *1* – reinforced soil massif, *2* – anchoring zone of reinforcement inserts, *3* – active zone of reinforced soil, *4* – casing of the front of the structure, *5* – tensile values of the reinforcement insert (*t* – along the insert's length, t_p – at the insert's connection spot (with retainment wall casing), *6* – value distribution of tensile forces along the length of the reinforcement insert, *7* – the line of maximum strain gauging at the level of the retainment wall, which divides the massif into the active and passive zone, *8* – the length of the insert's anchoring, *D* – the depth of the massif's foundation; $D \geq 0{,}4$ m – basic depth, $D = 0$ – in the event of the construction's resting on a rock or concrete

External stability is checked for the danger of the structure slipping along its base and the required bearing capacity of the ground. The structure is treated as a homogeneous mass loaded by internal and external forces. Internal loads are the dead weight of the massif, water buoyancy (if the structure is at risk of flooding) and inertia force (if the structure is located in an earthquake area). External loads include: pressure of the soil mass on the curtain wall (retaining wall), permanent and variable loads acting at the level of the massif floor and soil resistance forces. The pressure of the massif on the reinforced soil structure is calculated according to the scheme given in Figure 12 [6, 13].

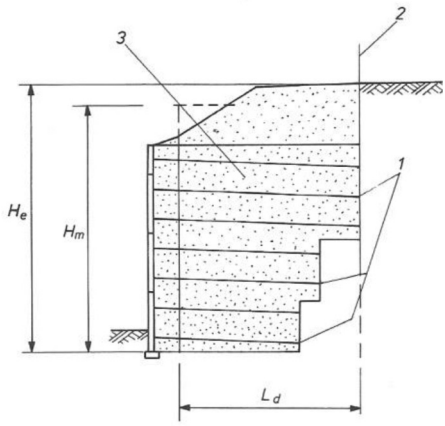

Fig. 12. Calculation scheme of the filling's pressure assumed in the event of external control of stability of the reinforced soil construction [6, 13]: *1* – actual tips of the reinforcement layers, *2* – the line of the reinforcement tips which determines the surface that is theoretically under the pressure of the organic soil filling which borders with the reinforcement soil construction, *3* – the zone of the external, active, vertical soil pressure onto the curtain wall, L_d – average length of reinforcement, H_e – total height of the reinforced soil construction

Internal stability examination consists in determining whether the strain gauging in the reinforcement are within the permissible range and whether the anchorage resistances of the inserts are greater than the forces pulling the reinforcement out of the soil material. Internal stability is checked according to a scheme developed on the basis of theoretical analyses and model tests, given in Figure 13 according to [6, 13].

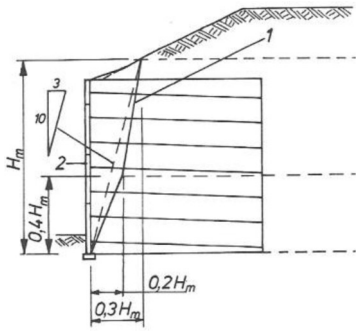

Fig. 13. Scheme of internal control of the stability of reinforced soil construction – vertical section through the reinforced massif characterised by height H_m [6, 13]: *1* – broken line representing the localization of maximum strain gauging within the reinforcement, *2* – construction casing (curtain wall)

In the case of general stability control (Fig. 14), the potential failure surfaces of the ground mass and the possibility of preventing landslides are considered, taking into account:

- the shear strength of the soil along these surfaces,
- strengthening of soil stability due to the installation of horizontal layers of reinforcement, crossed by the destruction surfaces.

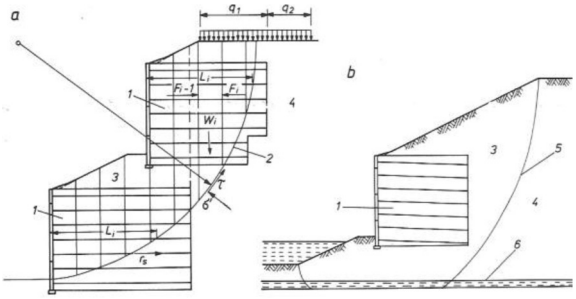

Fig. 14. Scheme of general stability control [6, 13]: *a* – damage along the cylindrical surface, *b* – individual example of massif's destruction, under which, there is a weak layer in the substrate, *1* – reinforcement soil massif, *2* – circular line of massif's destruction, *3* – the zone affected by destruction, *4* – the zone outside of destruction, *5* – (non-circular) line of massif's destruction, *6* – weak layer in the substrate, σ, τ – normal and tangential strain gauging acting on the surface of damaged massif, F_i – strain gauging present in the reinforcement layers cut by the damage surface, L_i – distance from the curtain wall to the point of intersection of the reinforcement layer by the damage surface

Fig. 14*a* applies to homogeneous soil, therefore the potential failure surface is assumed to be cylindrical in shape. However, the non-circular failure surface should be taken for a heterogeneous soil mass [6, 13]. If a heavy structure is supported on a mass of reinforced soil, then one possible form of destruction is a wedge-shaped splinter, encompassing the structure [6].

Control of the bearing capacity of the ground is to estimate the value of deformations that will occur after the construction of a reinforced soil structure. The causes of deformation of the reinforced mass may be internal or external (settlement and consolidation). Reinforcement is practically inextensible; thus, only external causes are considered in the design. The purpose of estimating settlements is to show that the deformations caused by them are within the acceptable range for reinforced soil structures and other structures within the range of influence of ground deformations.

CONCLUSION

Based on the model studies performed and the analysis of the test results, the following observations were made:

1. Estimating the size of the breakaway wedge in a physical model of a soil mass with horizontal reinforcement (and comparatively – in an unreinforced mass) is possible on the basis of looking for the maximum range of the zone of influence of the push of this wedge on the retaining wall of the model.
2. A reduction in the area of the soil wedge measuring 16÷49% was determined, depending on the number and type of reinforcement inserts (inserts with either "notched" or "smooth" surfaces were used) and soil compaction (either loosely embanked or pre-compacted soil mass was modelled).
3. It was found that the results of studies of the wedge of detachment by the method of searching for a zone in the ground massif, generating (due to the application of an external test load located on the roof of the massif) a horizontal thrust on the plane of the retaining wall of the model, coincided with the results of measurements of maximum tensile tensions in the inserts of the reinforcement by the method of electrical resistive strain gauging.
4. In a soil mass reinforced with bands of resistance elements (so-called "notches"), the effectiveness of the reinforcement depends minimally on the change in soil compaction. This rule is explained by the high quality of interaction of the inserts with the grains of the soil material (regardless of its level of compaction), determined by the resistance to displacement of the inserts.

5. In the case of a pre-densified massif reinforced with tapes with "smooth" surfaces, the effects of reinforcement are about 30% lower than in a loosely embanked massif. The reason for the weakened effectiveness is the slippage of the inserts relative to the grains of the soil medium.
6. For this reason, it is expedient to reinforce soil media that are loosened, characterized by a low value of the angle of internal friction φ and therefore exhibit significant and mostly uneven vertical displacements.
7. The results of the model studies presented in the article showed that in order to obtain the designed effect of reducing the area of the breakaway wedge, it is possible to use more than twice as many inserts of reinforcement with "notches" with respect to identical inserts with "smooth" surfaces.
8. The smaller the number of inserts used in the loose embankment massif, the greater the importance owing to the possibility of reducing the wedge of breakage is shown by the type of inserts (in relation to the value of friction on contact with the soil medium and the resistance of horizontal displacement of the inserts).

BIBLIOGRAPHY

[1] Bacot I., Lareal P.; Etude sur modeles reduits tridimensionneles de la nysture de massifs en terre armee. Bull. de liaison des Labo. Routiers Ponts et Chaussées, No. 60, 1972.

[2] Clayton C. R. J., Milititsky J., Woods R.J.; Earth Pressure and Earth Retaining Structures. Blackie Academic & Professional. An Im Print of Chapman & Hall. London-New York, 1996.

[3 Corte' J.; La methode des elements finis appliguee aux ouvrages en terre armee. Bulletin de Liaison des Laboratoire Routiers des Ponts et Chaussées, No 90, Juill-Aout, Paris 1977, pp. 37-48.

[4] Horvath J. S., Regins J., Colasanti P.E.; New hybrid subgrade model for soil structure interaction analysis; foundation and geosynthetics applications. ASCE Geo- Institute, Geo-Frontiers, March 2011.

[5] Ingold T. S. (ed.); The Practice of Soil Reinforcing in Europe. Thomas Telford, London 1996.

[6] Jarominiak A.; Lekkie konstrukcje oporowe. Wydawnictwa Komunikacji i Łączności, Warszawa 2010.

[7] Jones C. J. F. P.; Earth Reinforcement and Soil Structures. Thomas Telford, London 1996.

[8] Kulczykowski M., Leśniewska D.; Poradnik projektowania konstrukcji oporowych z gruntu zbrojonego. Prace IBW Polskiej Akademii Nauk, Gdańsk, 1996.

[9] Leśniewska D., Kulczykowski M.; Grunt zbrojony jako materiał kompozytowy. Podstawy projektowania konstrukcji. Wyd. IBW Polskiej Akademii Nauk, Gdańsk 2001.

[10] Long N. T., Schlosser F.; Zasada działania i zachowanie się gruntu zbrojonego - Wybrane zagadnienia geotechniki. Polska Akademia Nauk, IBW, Wrocław-Warszawa, Ossolineum, 1978, pp. 157-184.

[11] Long N. T.; Badania gruntów zbrojonych - Wybrane zagadnienia geotechniki. Polska Akademia Nauk, IBW, Wrocław-Warszawa, Ossolineum, 1978, pp. 185-210.

[12] Long N. T., Schlosser F.; Wymiarowanie murów z gruntów zbrojonych - Wybrane zagadnienia geotechniki. Polska Akademia Nauk, IBW, Wrocław-Warszawa, Ossolineum, 1978, pp. 211-237.

[13] NFP 94-200. Renforcement des sols par inclusions. Ouvrages en sols rapportes renforces par armatures ou nappes peu extensibles et souples. Dimensionnement.

[14] Sawicki A.; Statyka konstrukcji z gruntu zbrojonego. Wyd. IBW Polskiej Akademii Nauk, Gdańsk 1999.

[15] Sawicki A.; Mechanics of Reinforced Soil. A.A. Balkema, Rotterdam/Brookfield, 2000.

[16] Schlosser F.; La terre armee. Recherches et realisations. Bull. de Liaison des Labo. Routiers Ponts et Chaussées, No. 62, Nov.-Dec., 1972, pp. 79-92.

[17] Surowiecki A.; Multiscale modelling in railway engineering. Proc. of the XVI French-Polish Colloquium, Laboratoire de Mécanique & Génie Civil, Juillet 12-15, Montpellier 2013.

[18] Surowiecki A.; Komunikacyjne budowle ziemne ze wzmocnieniem skarp. Badania modelowe nośności i stateczności. Wyd. Wyższej Szkoły Oficerskiej Wojsk Lądowych im. gen. T. Kościuszki, Wrocław 2016, ISBN 978-83-65422-27-9.

[19] Surowiecki A.; Interaction between reinforced soil components. Studia Geotechnica et Mechanica, Vol. XX, No. 1-2, Wrocław 1998, pp. 43-61.

[20] Surowiecki A., Balawejder A.; Badanie możliwości wzmacniania nasypów kolejowych przy zastosowaniu zbrojenia gruntu, lekkich konstrukcji oporowych i maty komórkowej. Raport serii SPR nr 6. Projekt Bad. MNiI nr 5 T07E 06024, Politechnika Wrocławska, Instytut Inż. Ląd., Wrocław 2006.

[21] Wiłun Z.; Zarys geotechniki. Wydawnictwo Komunikacji i Łączności, Warszawa 2010.

[22] Zamiar Z.; Odbudowa infrastruktury transportowej [w:] Zbornik z 10 vedeckej konferencje Crisis Management, Zilinska Universite v Ziline, Slovak Republik 2006.

[23] Zamiar Z.; Infrastruktura transportu – wybrane zagadnienia. Wyd. Międzynarodowej Wyższej Szkoły Logistyki i Transportu, Wrocław 2011.

[24] Zamiar Z.; Infrastruktura transportu jako element infrastruktury krytycznej. Wyd. Międzynarodowej Wyższej Szkoły Logistyki i Transportu, Wrocław 2011. CL Consulting i Logistyka, Oficyna Wyd. NDiO.

[25] Zamiar Z., Bujak A.; Zarys infrastruktury i technologii przewozów podstawowych gałęzi transportu. Wyd. Międzynarodowej Wyższej Szkoły Logistyki i Transportu we Wrocławiu, Wrocław 2007.

[26] Zamiar Z., Surowiecki A., Saska P.; Infrastruktura transportowa. Bibl. Międzynarodowej Wyższej Szkoły Logistyki i Transportu we Wrocławiu, Ofic. Wyd. ATUT-Wrocławskie Wydawnictwo Oświatowe, Wrocław 2020.

Zenon Zamiar
The International University
of Logistics and Transport in Wroclaw, Poland
ORCID: 0000-0001-9887-0183
zzamiar@msl.com.pl

Andrzej Surowiecki
The International University
of Logistics and Transport in Wroclaw, Poland
ORCID: 0000-0003-4080-3409
andrzejsurowiecki3@wp.pl